

Magnetic-field-induced stress and magnetization in mechanically blocked Ni–Mn–Ga

N. N. Sarawate^{a)} and M. J. Dapino^{b)}

Department of Mechanical Engineering, The Ohio State University, Columbus, Ohio 43210, USA

(Received 21 January 2008; accepted 19 February 2008; published online 16 April 2008)

A single-crystal Ni–Mn–Ga sample (AdaptaMat, Ltd.) is first compressed from its longest shape to a given bias strain and subsequently subjected to a slowly alternating magnetic field while being prevented from deforming. The tests are repeated for several bias strains. The available blocking stress, or maximum field-induced stress relative to the bias stress, is critical for quantifying the work capacity of a material. The largest available blocking stress for this material is 1.47 MPa at a bias strain of 3% and field amplitude of 640 kA/m. The work capacity calculated as the area under the available blocking stress versus bias strain curve is 72.4 kJ/m³. An existing continuum thermodynamics model for Ni–Mn–Ga sensors is augmented by incorporating the magnetoelastic energy as a source of stress generation when the material is mechanically blocked. The strain and magnetization are described by fixing the variant volume fraction. © 2008 American Institute of Physics. [DOI: 10.1063/1.2904893]

I. INTRODUCTION

Due to their relatively large strain and broad frequency bandwidth, ferromagnetic shape memory alloys in the Ni–Mn–Ga system are mainly studied for actuation. Considerable experimental and modeling work has been done to describe this effect (see, e.g., review papers Refs. 1 and 2). Recently, the sensing behavior of Ni–Mn–Ga was experimentally investigated,³ and a continuum thermodynamics model was presented to simultaneously describe the sensing and actuation effects.^{4,5} The actuation effect is described by the dependence of strain and magnetization on magnetic field at constant stress, and the sensing effect is described by the dependence of stress and magnetization on strain at constant magnetic field.

The force generated by a Ni–Mn–Ga sample under partially blocked conditions during actuation measurements was presented by Henry⁶ and O’Handley *et al.*⁷ Their measurements suggest the presence of significant magnetoelastic coupling: as the transverse magnetic field was increased below the field required to initiate twin boundary motion, the measured stress increased even though the sample and spring remained undeformed. Because a spring was used to precompress the sample in the axial direction, some amount of detwinning was allowed and hence, the blocking stresses were not measured. Further, no model for magnetization was presented. Force measurements under completely mechanically blocked conditions at different bias strains were presented by Jaaskelainen *et al.*⁸ and recently by Couch and Chopra.⁹ Neither magnetization measurements nor analytical models were included. Likhachev *et al.*¹⁰ presented an expression for the thermodynamic driving force induced by magnetic fields acting on the twin boundary. This force depends on the derivative of the magnetic energy difference between the hard axis

and easy axis configurations. Although this force is useful in modeling the strain versus field and stress versus strain, its origin is not well understood. This force is independent of the volume fraction, and thus it cannot accurately model the stress versus field behavior in which the net generated stress varies with bias strain (see Fig. 4).

The available blocking stress, defined as the maximum field-induced stress relative to the bias stress, is critical for quantifying the work capacity of an active material. In this study we characterize and model the magnetic-field-induced stress and magnetization generated by a commercial Ni–Mn–Ga sample (AdaptaMat, Ltd.) when it is prevented from deforming. We refer to this type of mechanical boundary as a “mechanically blocked condition.” The material is first compressed from its longest shape to a given bias strain (which requires a corresponding bias stress) and is subsequently subjected to a slowly alternating magnetic field while being prevented from deforming. The tests are repeated for several bias strains.

A previous continuum thermodynamics model⁴ is used to model the dependence of stress and magnetization on the applied field and bias strain. The magnetic Gibbs energy is used as a thermodynamic potential with contributions from Zeeman, anisotropy, magnetostatic, and elastic strain energies. The microstructure of Ni–Mn–Ga is included in the thermodynamic framework by means of the internal state variables variant volume fraction, domain fraction, and magnetization rotation angle. The invariance of the strain under mechanically blocked conditions is modeled by fixing the variant volume fraction. The magnetoelastic energy is not considered while evaluating the domain fraction and magnetization rotation angle because it is around 1000 times smaller than the Zeeman, magnetostatic, and anisotropy energies. On the other hand, the magnetoelastic energy becomes significant as it is the sole source of stress generation when field-induced deformations are prevented.

^{a)}Electronic mail: sarawate.1@osu.edu.

^{b)}Author to whom correspondence should be addressed. Electronic mail: dapino.1@osu.edu.

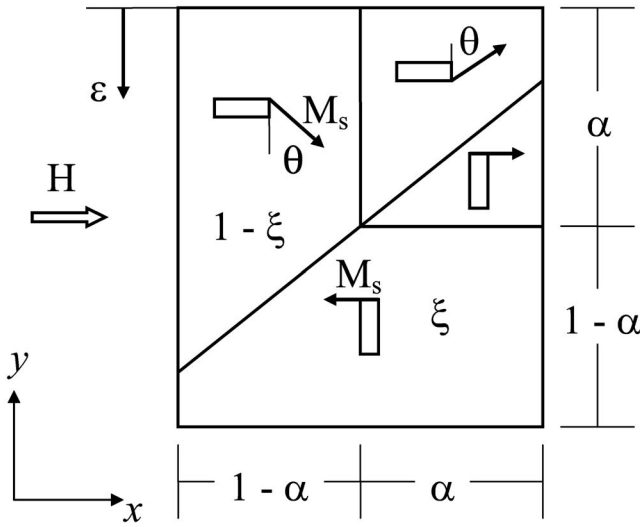


FIG. 1. Simplified two-variant Ni-Mn-Ga microstructure.

II. EXPERIMENT

Our experimental setup consists of a custom-made electromagnet and a uniaxial stress stage. A $6 \times 6 \times 10 \text{ mm}^3$ Ni-Mn-Ga sample (AdaptaMat, Ltd.) is placed in the center gap of the electromagnet. The sample exhibits a free magnetic-field-induced deformation of 5.8% under a transverse field of 700 kA/m. The material is first converted to a single field-preferred variant by applying a high transverse field and is subsequently compressed to a desired bias strain. The sample is then subjected to a sinusoidal transverse field of amplitude 700 kA/m and frequency of 0.25 Hz. A $1 \times 2 \text{ mm}^2$ transverse Hall probe placed in the gap between a magnet pole and the face of the sample measures the flux density from which the magnetization inside the sample is obtained after accounting for demagnetization fields. The compressive force is measured by a 200 pounds of force (lbf) load cell, and the displacement is measured by a linear variable differential transducer. This process is repeated for several bias strains ranging between 1 and 5.5%.

III. MODELING

The presented model builds on an existing sensing model⁴ which uses the continuum thermodynamics approach to describe the dependence of stress and magnetization on external strain at constant bias field. To model the stress-associated magnetoelastic coupling in mechanically blocked condition, the model is modified by adding magnetoelastic energy and assuming constant variant volume fraction. Figure 1 shows an ideal two-variant Ni-Mn-Ga microstructure¹¹ consisting of a field-preferred variant (ξ) and a stress-preferred variant ($1 - \xi$). In each variant, the magnetic domains ($\alpha, 1 - \alpha$) are generated to minimize the net magneto-static energy. The applied magnetic field is oriented in the x direction, and the magnetization vectors in the field-preferred variant are oriented either in the direction of the field or opposing it. However, the magnetization vectors in the stress-preferred variants can rotate by an angle θ , which is equal and opposite in the two domains. The complete model

development is given in Ref. 4. The key components of the model and essential modifications to account for the magnetoelastic coupling are given here.

The Clausius–Duhem inequality states that the rate of change of entropy is greater than or equal to the entropy increase rate due to the specific heat supply rate minus the entropy decrease rate due to the heat flux vector. When combined with the first law of thermodynamics, the Clausius–Duhem inequality takes the local form

$$-\rho\dot{\psi} - \rho\eta\dot{\Theta} + \mathbf{P} \cdot \dot{\mathbf{F}} + \mu_0 \vec{\mathbf{H}} \cdot \dot{\vec{\mathbf{M}}} - \frac{1}{\Theta} \mathbf{q} \cdot \text{grad } \Theta \geq 0, \quad (1)$$

where ψ is the specific Helmholtz energy, ρ is the density of the material in referential coordinates, η is the specific entropy, Θ is the absolute temperature, \mathbf{P} is the first Piola Kirchhoff stress tensor, \mathbf{F} is the deformation gradient tensor, and \mathbf{q} is the heat flux vector representing the heat leaving the system. The term $\mathbf{P} \cdot \dot{\mathbf{F}}$ represents the stress power, or the rate of work done on the material by external mechanical forces.

The term $\mu_0 \vec{\mathbf{H}} \cdot \dot{\vec{\mathbf{M}}}$ represents the rate of work done on the material by a magnetic field,¹² with $\vec{\mathbf{H}}$ denoting the applied magnetic field vector and $\vec{\mathbf{M}}$ the net magnetization vector.

For the case under consideration, the externally applied bias strain ε and engineering stress σ are oriented along the longitudinal (y) axis of the sample. The applied field H and net magnetization M are oriented along the transverse (x) axis of the sample. As in the sensing case,⁴ the applied field H is an independent variable. Therefore, a magnetic Gibbs energy potential φ is defined through the Legendre transform

$$\rho\varphi = \rho\psi - \mu_0 H M. \quad (2)$$

Assuming isothermal conditions ($\dot{\Theta} = 0$ and $\text{grad } \Theta = 0$) and using Eqs. (1) and (2), a modified Clausius–Duhem inequality is obtained,

$$-\rho\dot{\varphi} + \sigma\dot{\varepsilon} - \mu_0 \dot{H} M \geq 0. \quad (3)$$

The total magnetic Gibbs energy is the sum of the mechanical and magnetic (Zeeman, magnetostatic, and anisotropy) contributions of the two variants,

$$\begin{aligned} \rho\varphi = & \frac{1}{2} E \varepsilon_e^2 + \xi \left[-\mu_0 H M_s \alpha + \mu_0 H M_s (1 - \alpha) \right. \\ & \left. + \frac{1}{2} \mu_0 N [M_s \alpha - M_s (1 - \alpha)]^2 \right] + (1 - \xi) \\ & \times \left[-\mu_0 H M_s \sin \theta + \frac{1}{2} \mu_0 N M_s^2 \sin^2 \theta + K_u \sin^2 \theta \right], \end{aligned} \quad (4)$$

where M_s is saturation magnetization. The parameters needed for quantification of the mechanical energy are obtained from the experimental stress versus strain curve at zero bias field. The total strain (ε) is considered as the sum of elastic (ε_e) and detwinning (ε_{tw}) components; the latter is given by $\varepsilon_0(1 - \xi)$, with ε_0 being the lattice distortion (5.8%). The elastic modulus E is the average of the minimum and maximum moduli, which are obtained with the material in

single variant preferred by field and stress, respectively. Parameter N is the difference between the transverse and longitudinal demagnetization factors.^{4,13} The anisotropy constant K_u is evaluated experimentally as the difference in the area of the easy axis and hard axis magnetization curves, since it represents the energy associated with pure rotation of the magnetization vectors. Following the classical Coleman–Noll procedure, Eq. (3) takes the form

$$\left[\sigma - \frac{\partial(\rho\varphi)}{\partial\varepsilon} \right] \dot{\varepsilon} + \left[-\mu_0 M - \frac{\partial(\rho\varphi)}{\partial H} \right] \dot{H} + \pi^\alpha \dot{\alpha} + \pi^\theta \dot{\theta} + \pi^\xi \dot{\xi} \geq 0, \quad (5)$$

where the terms $\pi^\alpha = -\partial(\rho\varphi)/\partial\alpha$, $\pi^\theta = -\partial(\rho\varphi)/\partial\theta$, and $\pi^\xi = -\partial(\rho\varphi)/\partial\xi$ represent thermodynamic driving forces associated with internal state variables α , θ , and ξ , respectively. This leads to the constitutive equations

$$\sigma = \frac{\partial(\rho\varphi)}{\partial\varepsilon} = E(\varepsilon - \varepsilon_{tw}), \quad (6)$$

$$M = -\frac{1}{\mu_0} \frac{\partial(\rho\varphi)}{\partial H} = M_s [(2\alpha - 1)\xi + \sin\theta(1 - \xi)]. \quad (7)$$

Because the easy and hard axis magnetization curves of Ni–Mn–Ga show negligible hysteresis, the evolution of the domain fraction (α) and rotation angle (θ) is assumed to be reversible. Hence, the driving forces are zero; $\pi^\alpha = 0$ and $\pi^\theta = 0$. This gives closed form solutions for the variables α and θ ,

$$\alpha = \frac{1}{2} + \frac{H}{2NM_s}, \quad (8)$$

$$\theta = \arcsin\left(\frac{\mu_0 HM_s}{\mu_0 NM_s^2 + 2K_u}\right). \quad (9)$$

The Clausius–Duhem inequality, Eq. (5), is thus reduced to

$$\pi^\xi \dot{\xi} \geq 0. \quad (10)$$

In the actuation and sensing model, the volume fraction is numerically evaluated by using a critical yield function π^{cr} which represents the energy barrier to initiate detwinning.^{4,5} Since in this study the sample is prevented from deforming, it is assumed that the volume fraction remains unchanged after the initial compression when the field is applied. The amount of twin reorientation that may occur is assumed to be negligible. The initial volume fraction and stress at zero field and given bias strain are calculated using the sensing model.⁴

The magnetoelastic coupling is often ignored in the modeling of actuation and sensing in Ni–Mn–Ga, in which the strains due to variant reorientation are considerably larger than the magnetostrictive strains. This has been experimentally confirmed by Heczko¹⁴ and Tickle and James.¹⁵ The magnetoelastic energy is also ignored in the calculation of the magnetic parameters through Eqs. (8) and (9), as its contribution is around 3 orders of magnitude smaller than the other magnetic energy terms. However, the contribution of the magnetoelastic coupling toward the generation of stress in mechanically blocked conditions is significant: twin

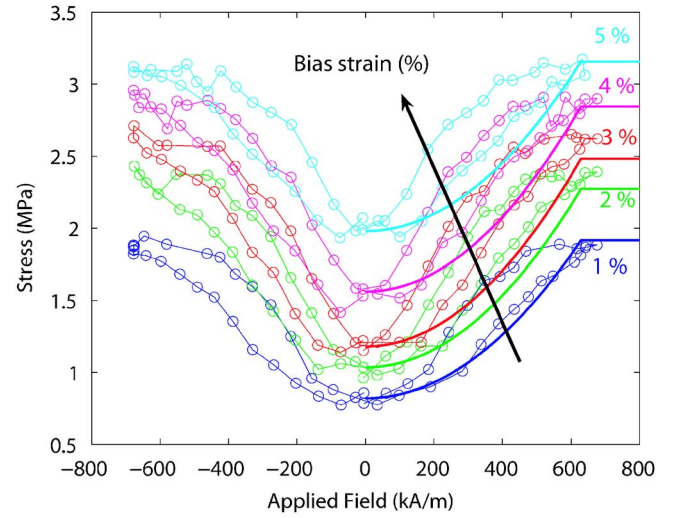


FIG. 2. (Color online) Stress vs magnetic field at several bias strains. Dots: experiment; solid line: model.

boundary motion is completely suppressed and the magnetoelastic energy is the sole source of stress generation when a magnetic field is applied. The magnetoelastic energy is proposed as

$$\rho\varphi_{me} = B_1 \varepsilon_y (1 - \xi) (-\sin^2 \theta) + \sigma_0 \varepsilon_y \xi (-\sin^2 \theta). \quad (11)$$

Here, B_1 represents the magnetoelastic coupling coefficient,¹³ obtained by measuring the maximum stress generated when the sample is biased by 5.5% (when $\xi = 0$), and ε_y represents the magnetorestriction in the y direction. The first term represents the magnetoelastic energy contribution due to magnetic fields, which is nonzero only in the stress-preferred variant ($1 - \xi$). The second term represents the energy contribution due to the initial compressive stress σ_0 . The applied field leads to increase of energy in stress-preferred variants, whereas the stress leads to increase of energy in field-preferred variants. The stress generated by magnetoelastic coupling thus has the form

$$\sigma_{me}(H) = [B_1(1 - \xi) + \sigma_0 \xi] (-\sin^2 \theta). \quad (12)$$

IV. RESULTS

Figure 2 shows experimental and calculated stress versus applied field curves at varied bias strains. Hysteresis is not included in the model. The significance of magnetoelastic coupling is evident as the stress starts increasing as soon as the field is applied, with the rotation of magnetization vectors. The increase in stress is directly related to the angle of rotation (θ) predicted by the magnetization model. On the contrary, the variant reorientation process is typically associated with a high amount of coercive field that increases with increasing bias stress.^{4,16} The absence of a coercive field, and of discontinuity in stress profiles, confirms the magnetoelastic coupling rather than twin reorientation as the origin of the stress.

Figure 3 shows the magnetization dependence on applied field at varied bias strains. The negligible hysteresis is typical of single-crystal Ni–Mn–Ga when the volume fraction is approximately constant. Thus, the model assumption

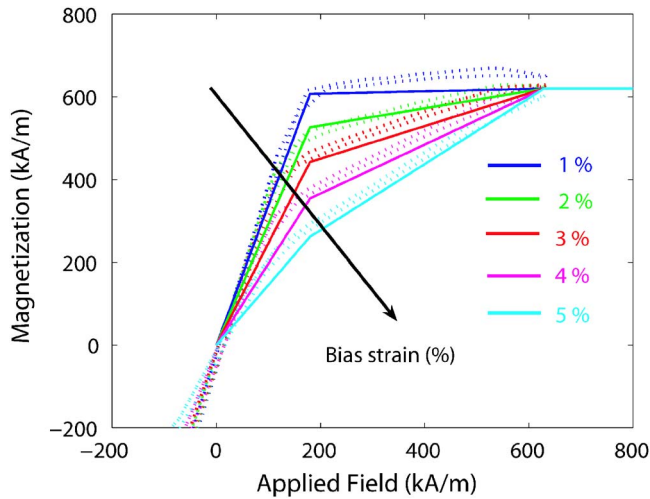


FIG. 3. (Color online) Magnetization vs field at several bias strains. Dashed line: experiment; solid line: model.

of reversible evolution of α and θ is validated along with the assumption of constant volume fraction. A good agreement is observed between the experimental results and model simulations. The model parameters are $E=3$ GPa, $N=0.2$, $M_s=605$ kA/m, $K_u=1.67 \times 10^5$ J/m³, and $B_1=1$ MPa.

Figure 4 shows the blocking stress σ_{bl} (stress at 700 kA/m in Fig. 2), minimum stress σ_0 (stress at zero field in Fig. 2), and available blocking stress $\sigma_{bl}-\sigma_0$ as a function of bias strain. The largest available blocking stress is 1.47 MPa at 3% bias strain and field of 700 kA/m. At 3% strain, the material consists of an almost equal contribution of the two variant volume fractions.

V. DISCUSSION

Our mechanically blocked measurements and thermodynamic model for constant volume fraction describe the stress

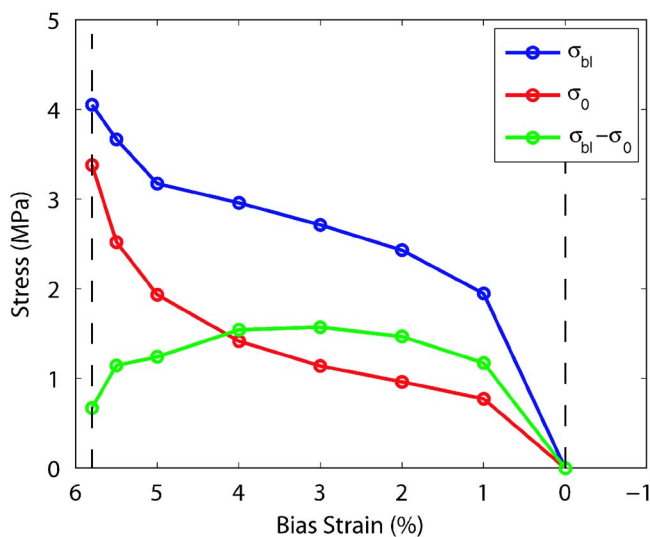


FIG. 4. (Color online) Experimental blocking stress σ_{bl} , minimum stress σ_0 , and available blocking stress $\sigma_{bl}-\sigma_0$ vs bias strain.

and magnetization dependence on field and provide a measure of the work capacity of Ni-Mn-Ga. The work capacity, defined as the area under the $\sigma_{bl}-\sigma_0$ curve, is 72.4 kJ/m³ for this material. This value compares favorably with that of Terfenol-D and PZT (18–73 kJ/m³, Ref. 17). However, the work capacity of Ni-Mn-Ga is strongly biased toward high deformations at the expense of low generated forces, which severely limits the actuation authority of the material. Terfenol-D exhibits a measured stress of 8.05 MPa at a field of 25 kA/m and prestress of -6.9 MPa.¹⁸ The lower blocking stress of 1.47 MPa produced by Ni-Mn-Ga is attributed to a low magnetoelastic coupling.

The maximum *available* blocking stress is observed at a bias strain of 3%, though the maximum blocking stress occurs, as expected, when the sample is completely prevented from deforming. Due to the competing effect of the stress-preferred and field-preferred variants, the stress is highest when the volume fractions are approximately equal ($\xi=0.5$).

The magnetoelastic energy in Ni-Mn-Ga is considerably smaller than the Zeeman, magnetostatic, and anisotropy energies. The magnetostrictive strains in Ni-Mn-Ga are of the order of 50–300 ppm,^{14,15} which are negligible when compared to the typical 6% deformation that occurs by twin-variant reorientation. The contribution of magnetoelastic coupling can thus be ignored when describing the sensing and actuation behaviors in which the material deforms by a several percent strain. In the special case of field application in mechanically blocked condition, twin-variant reorientation is completely suppressed and the magnetoelastic coupling becomes significant as it remains the only source of stress generation. This is validated from the experimental stress data as there is no coercive field associated with the twin-variant rearrangement. In summary, the magnetoelastic coupling in Ni-Mn-Ga is relatively low but becomes significant when the material is prevented from deforming.

¹O. Soderberg, Y. Ge, A. Sozinov, S. Hannula, and V. Lindroos, *Smart Mater. Struct.* **14**, S223 (2005).

²J. Kiang and L. Tong, *J. Magn. Magn. Mater.* **292**, 394 (2005).

³N. Sarawate and M. Dapino, *Appl. Phys. Lett.* **88**, 121923 (2006).

⁴N. Sarawate and M. Dapino, *J. Appl. Phys.* **101**, 123522 (2007).

⁵N. Sarawate and M. Dapino, *Proc. SPIE* **6526**, 652629 (2007).

⁶C. Henry, Ph.D. Thesis, Massachusetts Institute of Technology (2002).

⁷R. O'Handley, S. Allen, P. David, C. Henry, M. Marioni, D. Bono, and C. Jenkins, *Proc. SPIE* **5053**, 200 (2003).

⁸A. Jaaskelainen, K. Ullakko, and V. Lindroos, *J. Phys. IV* **112**, 1005 (2003).

⁹R. Couch and I. Chopra, *Proc. SPIE* **6173**, 42 (2006).

¹⁰A. Likhachev, A. Sozinov, and K. Ullakko, *Mater. Sci. Eng.* **378**, 513 (2004).

¹¹O. Heczko, *J. Magn. Magn. Mater.* **290–291**, 787 (2005).

¹²Y. Pao and K. Hutter, *Proc. IEEE* **63**, 1011 (1975).

¹³R. O'Handley, *Modern Magnetic Materials: Principles and Applications* (Wiley-Interscience, New York, 2000).

¹⁴O. Heczko, *J. Magn. Magn. Mater.* **290–291**, 846 (2005).

¹⁵R. Tickle and R. James, *J. Magn. Magn. Mater.* **195**, 627 (1999).

¹⁶B. Kiefer and D. Lagoudas, *Philos. Mag.* **85**, 4289 (2005).

¹⁷V. Giurgiutiu, C. Rogers, Z. Chaudhry, and J. Intel, *J. Intell. Mater. Syst. Struct.* **7**, 4 (1996).

¹⁸M. Dapino, R. Smith, L. Faidley, A. Flatau, and J. Intel, *J. Intell. Mater. Syst. Struct.* **11**, 135 (2000).